Geophysical Research Letters

RESEARCH LETTER
10.1029/2022GL098625

Holocene Multi-Centennial Variations of the Asian Summer Monsoon Triggered by Solar Activity

Weiyi Sun[1], Jian Liu[1,2,3], Bin Wang[4], Deliang Chen[5], Lingfeng Wan[6], and Jing Wang[1]

[1]Key Laboratory for Virtual Geographic Environment, Ministry of Education, State Key Laboratory Cultivation Base of Geographical Environment Evolution of Jiangsu Province, Jiangsu Center for Collaborative Innovation in Geographical Information Resource Development and Application, School of Geography Science, Nanjing Normal University, Nanjing, China, [2]Jiangsu Provincial Key Laboratory for Numerical Simulation of Large Scale Complex Systems, School of Mathematical Science, Nanjing Normal University, Nanjing, China, [3]Open Studio for the Simulation of Ocean-Climate-Isotope, Qingdao National Laboratory for Marine Science and Technology, Qingdao, China, [4]Department of Atmospheric Sciences and Atmosphere-Ocean Research Center, University of Hawaii at Manoa, Honolulu, HI, USA, [5]Regional Climate Group, Department of Earth Sciences, University of Gothenburg, Gothenburg, Sweden, [6]Institute of Advanced Ocean Study, Ocean University of China, Qingdao, China

Key Points:

- Transient Holocene simulation and proxies show that Asian summer monsoon (ASM) has a significant multi-centennial (300–600 year) variation since the mid-Holocene
- ASM multi-centennial variability is primarily influenced by the western North Pacific (WNP) circulation anomalies that changes tropical Asian monsoon trough
- Solar activity modulates tropical Pacific sea surface temperature and instigates an anomalous WNP cyclone, causing a delayed ASM increase

Supporting Information:

Supporting Information may be found in the online version of this article.

Correspondence to:

J. Liu,
jliu@njnu.edu.cn

Citation:

Sun, W., Liu, J., Wang, B., Chen, D., Wan, L., & Wang, J. (2022). Holocene multi-centennial variations of the Asian summer monsoon triggered by solar activity. *Geophysical Research Letters*, *49*, e2022GL098625. https://doi.org/10.1029/2022GL098625

Received 10 MAR 2022
Accepted 28 JUN 2022

Author Contributions:

Conceptualization: Weiyi Sun, Jian Liu
Formal analysis: Weiyi Sun, Lingfeng Wan
Methodology: Weiyi Sun, Lingfeng Wan, Jing Wang
Software: Weiyi Sun
Supervision: Bin Wang
Validation: Weiyi Sun, Jing Wang
Writing – original draft: Weiyi Sun

Abstract Solar activity affects Asian summer monsoon (ASM) at various time scales. However, it remains unknown if and how solar activity can influence ASM on the centennial time scale. Using the Community Earth System Model, we conduct a solar activity forced Holocene transient simulation with an acceleration factor of 10 and show that during the middle–late Holocene ASM precipitation exhibits a significant 300–600-year periodicity under solar forcing. This model-produced multi-centennial variation is also suggested by proxy data. The leading mode of the multi-centennial ASM variation shows a "wet tropics–dry subtropics" pattern, which lags the corresponding solar activity by about a quarter cycle. The western North Pacific (WNP) circulation system is responsible for the multi-centennial ASM variation, through enhancing the climatological south Asia–WNP monsoon trough. We suggest that solar activity modulates the zonal SST gradients of the tropical Pacific, inducing the anomalous WNP cyclone and enhancing ASM precipitation in a delayed mode.

Plain Language Summary More than 300 years have passed since the last solar minimum (Maunder grand solar minima, ~1,650–1,715), and now we are around the maximum solar period. This means that the centennial solar cycle may potentially influence the past, recent, and future climate. However, due to the limited temporal length of instrumental data and the scattered spatial distribution of reconstructions, if and how solar activity can influence Asian summer monsoon (ASM) on the centennial time scale is under debate. This study carried out the Holocene transient simulation under solar activity forcing for the first time, using the Community Earth System Model (CESM). We found that the ASM exhibits a significant 300–600-year periodicity under solar forcing during the middle–late Holocene. The leading mode of the multi-centennial ASM variation shows a "wet tropics–dry subtropics" pattern, which lags solar activity by about a quarter cycle. The physical process is that solar activity modulates the ENSO-like sea surface temperature over tropical Pacific, developing an anomalous western North Pacific cyclone, which causes a delayed ASM precipitation change. These findings may have implications for predicting the influence of the anticipated future solar activity on the Asian monsoon system.

1. Introduction

The Asian monsoon is one of Earth's most active climate systems, with considerable air–sea–land interaction, and plays an important role in global water and energy cycles. It has been established that the interannual-interdecadal variations of Asian summer monsoon are primarily driven by the internal variability of the coupled climate system, such as the El Niño–Southern Oscillation (ENSO), the Pacific Decadal Oscillation, the Atlantic Multidecadal Oscillation (e.g., Dong & Ding, 2016; Goswami et al., 2006; Lu et al., 2006; Wang et al., 2000). The role of the anthropogenic forcing on the trend of Asian monsoon has also been extensively investigated (Wang et al., 2021). However, there are relatively few studies on the low-frequency Asian monsoon variability under natural external forcings, and the associated mechanisms remain elusive.

Observations have shown significant statistical correlations between the 11-year solar cycle and the climate system. For example, the Coupled Model Inter-comparison Project 5 (CMIP5) simulations and HadCRUT4 data

Writing – review & editing: Weiyi Sun, Jian Liu, Bin Wang, Deliang Chen

showed that the global mean temperature change lags behind solar activity by approximately 1–2 years (Misios et al., 2016). In the Pacific region, a La Niña-like state occurred in the peaks of 11-year solar variability, while an anomalous equatorial Pacific warming was found a few years after each peak (Meehl & Arblaster, 2009; Meehl et al., 2009). However, due to the limited temporal length of observations, less attention has been paid to centennial solar variability.

Studies of the high-resolution global reconstructions of temperature and precipitation during the past 2,000 years suggested a significant 200-year climatic cycle with a lagged response to the solar activity by 0–20 years; these include proxies from Qinghai, central Asia, and continental Siberian Altai (Breitenmoser et al., 2012). J. Liu et al. (2009), Z. Liu et al. (2009) documented a quasi-bicentennial oscillation in global monsoon precipitation during the last millennium, caused by changes in the land–sea thermal contrast and hemispheric temperature gradient induced by the 200-year solar cycle (de Vries cycle). This de Vries cycle has been widely found in the $\Delta^{14}C$ and ^{10}Be records (e.g., Wagner et al., 2001). Additionally, studies has also investigated the impacts of the de Vries cycle on drought events over eastern China (Sun et al., 2017), global ocean temperature (Seidenglanz et al., 2012), and the Intertropical Convergence Zone (Novello et al., 2016).

The solar irradiance reconstruction for the past 10 ka suggests that in addition to the 200-year periodicity, there exists about 500-year cycle of solar activity (Steinhilber et al., 2012; Vieira et al., 2011). Considerable 500-year variability was found in the dry/wet records over the Asian monsoon region, such as the proxies over Northeast China (Xu et al., 2019), Eastern China (Wang et al., 2005), South Korea (Park, 2017), southern Qinghai-Tibet Plateau (Sun et al., 2020), which was suggested to be associated with solar activity. For example, solar activity leads the $\delta^{18}O$ record from Dongge cave by about 22 years (Steinhilber et al., 2012) and leads Indian monsoon precipitation by a few hundred years (Tiwari et al., 2015). Some studies also found a significant ∼500-year cycle of the ENSO variance, coincident with periodic solar activity, further affecting the Asian summer monsoon (ASM) (Zhu et al., 2017). However, restricted by the uneven and scattered spatial distribution of reconstructions, the knowledge of ASM's multi-centennial variability has been limited on regional scales. Proxy data–model comparison is needed to better understand the evolution, spatial characteristics, and dynamic mechanisms of multi-centennial climate variability. Previous modeling work has mainly focused on the climatic trend during the Holocene (e.g., Cheng et al., 2021; Liu et al., 2014; Sun, Wang, et al., 2019); however, analysis of multi-centennial ASM variability remains a missing area of study, and solar activity forcing is also rarely considered in Holocene transient simulations. How the multi-centennial solar activity (∼500 years) affects the ASM variability remains unknown.

The present study aims to address the following questions: (a) What are the spatiotemporal characteristics of ASM variation on the multi-centennial time scale during the Holocene? (b) Could solar activity drive multi-centennial ASM changes? (c) If so, how does solar activity affect the ASM multi-centennial variation? Here we used high-resolution dry/wet proxies over the ASM region and conducted Holocene transient experiments with an acceleration factor of 10 under orbital forcing and solar activity forcing to detect the responses of the ASM to the total solar irradiance (TSI) and understand the underlying physical processes.

2. Methods

2.1. Model Simulation

This study used the Community Earth System Model 1 (CESM1), with a resolution of T31_g37. The atmospheric model (CAM) had a global range of 48 × 96 grids and 26 vertical levels, while the oceanic model (POP) had a range of 116 × 100 grids with 60 vertical levels. A control (Ctrl) experiment was conducted to run for 1,550 years based on pre-industrial (PI) background conditions. The simulated global precipitation, temperature, atmospheric circulation, and ENSO variability were similar to observed data (e.g., Sun, Liu et al., 2019).

Next, we set the Earth's orbital parameters to the values of 12 ka BP and conducted a 400-year spin-up run, starting at the equilibrium state of the Ctrl experiment. Then, we performed an orbital forcing (ORB) experiment, forced by the Earth's orbital parameters varying from 12 to 0 ka BP. It should be noted that an acceleration factor of 10 was used for varying the orbital parameters (Lorenz & Lohmann, 2004), so the duration of the ORB experiment was 1,200 model years. Similarly, we added the solar forcing and ran another experiment (ORB + TSI), varying both orbital parameters and total solar irradiance (Figure S2a in Supporting Information S1); an acceleration factor of 10 was again applied. Because the time length of the solar forcing we used was about the last

11.5 ka (Vieira et al., 2011), the ORB + TSI experiment was run from 11 to 0 ka BP. The original solar forcing is 10-year resolution. Following the transient modeling work by He et al. (2021), we used the ORB + TSI minus ORB experiments to isolate the net effect of solar activity (TSI).

Additionally, we also used the simulation of transient climate evolution over the last 21,000 years (TraCE-21ka) for comparison (J. Liu et al., 2009, Z. Liu et al., 2009). The TraCE-21ka contains five experiments, including four single forcing sensitivity experiments of Earth orbital parameters, greenhouse gases, ice sheets, and meltwater, plus an all-forcing experiment driven by these four external forcings.

2.2. Study Area and Proxy Data

The instrumental data included monthly mean precipitation from the Global Precipitation Climatology Project version 2.3 (Adler et al., 2003). The Asian monsoon precipitation domain was computed using the last 30 years of climatology from the GPCP. Specifically, the ASM region was defined by the Asian region where the May–September (local summer) mean precipitation minus the November–March (winter) mean precipitation exceeded 2 mm day^{-1}, and the May–September precipitation exceeded 55% of annual precipitation (Wang & Ding, 2008).

We also collected high temporal resolution dry/wet proxy data over the Asian monsoon region, which were compiled from the published literature (Table S1 in Supporting Information S1). The temporal resolutions of these data were approximately equal to, or less than, several decades, which was sufficient to reflect climatic variability on a centennial time scale. Proxy data were linearly interpolated to 10-year resolution, and data of Dykoski et al. (2005), Tiwari et al. (2015), Wang et al. (2005), and Zhu et al. (2017) were multiplied by negative 1 to represent wet condition.

2.3. Extracting Signals of Multi-Centennial Variation

To extract the 300–600-year multi-centennial frequencies, a method of subtracting the 400-year running mean from the 150-year running mean was applied to the modeling results. Compared with the 300–600-year bandpass filtered data, we found our method better preserved the multi-centennial power and magnitude, consistent with previous studies (Shi et al., 2019). Statistical tests for the correlation and regression were based on the effective degrees of freedom (Bretherton et al., 1999).

3. Results

3.1. Spatiotemporal Variations of ASM on the Multi-Centennial Time Scale

The multi-centennial periodicities of the ASM and their spatial distribution were examined using proxy data reconstructions (Figure 1). Most of the proxy records suggested a multi-centennial variation with a relatively broad range of energy peaks ranging from 300 to 600 years. Examples included the proxies over northeast Asia (Li et al., 2020; Xu et al., 2019), southeastern China (Huang et al., 2019; Wang et al., 2005), the southern Qinghai–Tibet Plateau (Ming et al., 2020; Sun et al., 2020), and the Indian monsoon regions (Tiwari et al., 2015) (Figure 1a). In central China, quasi-millennial (~800–961 years) (Tan et al., 2018; Zhang et al., 2020) and quasi-bicentennial cycles (Zhang et al., 2013) were found (Table S1 in Supporting Information S1), which might be related to the Eddy cycle (~1,000 years) and de Vries cycle (~200 years), respectively (Bond et al., 2001; Wagner et al., 2001). Meanwhile, the time range of eight of the sets of proxy data was from the middle Holocene to late Holocene, and seven sets showed marked multi-centennial periodicities (Table S1 in Supporting Information S1). We also divided other proxies into early–mid and mid–late Holocene, and found stronger multi-centennial periodicities of 300–600 years during the mid–late Holocene, compared with the early–mid Holocene (Figure S1 in Supporting Information S1); these might be associated with enhanced multi-centennial variability of solar activity (Figure S2 in Supporting Information S1).

To identify the effect of solar activity contributing to multi-centennial ASM variability, we investigated the simulated summer (June–July–August, JJA) mean ASM land precipitation in the ORB and TSI experiments. The precipitation generally showed few multi-centennial signals in the ORB (Figure 2a–2c) and Ctrl experiments, suggesting that orbital forcing and its modulated internal variability are not able to reproduce multi-centennial ASM variability. However, under TSI, the ASM precipitation displayed significant peaks on approximately

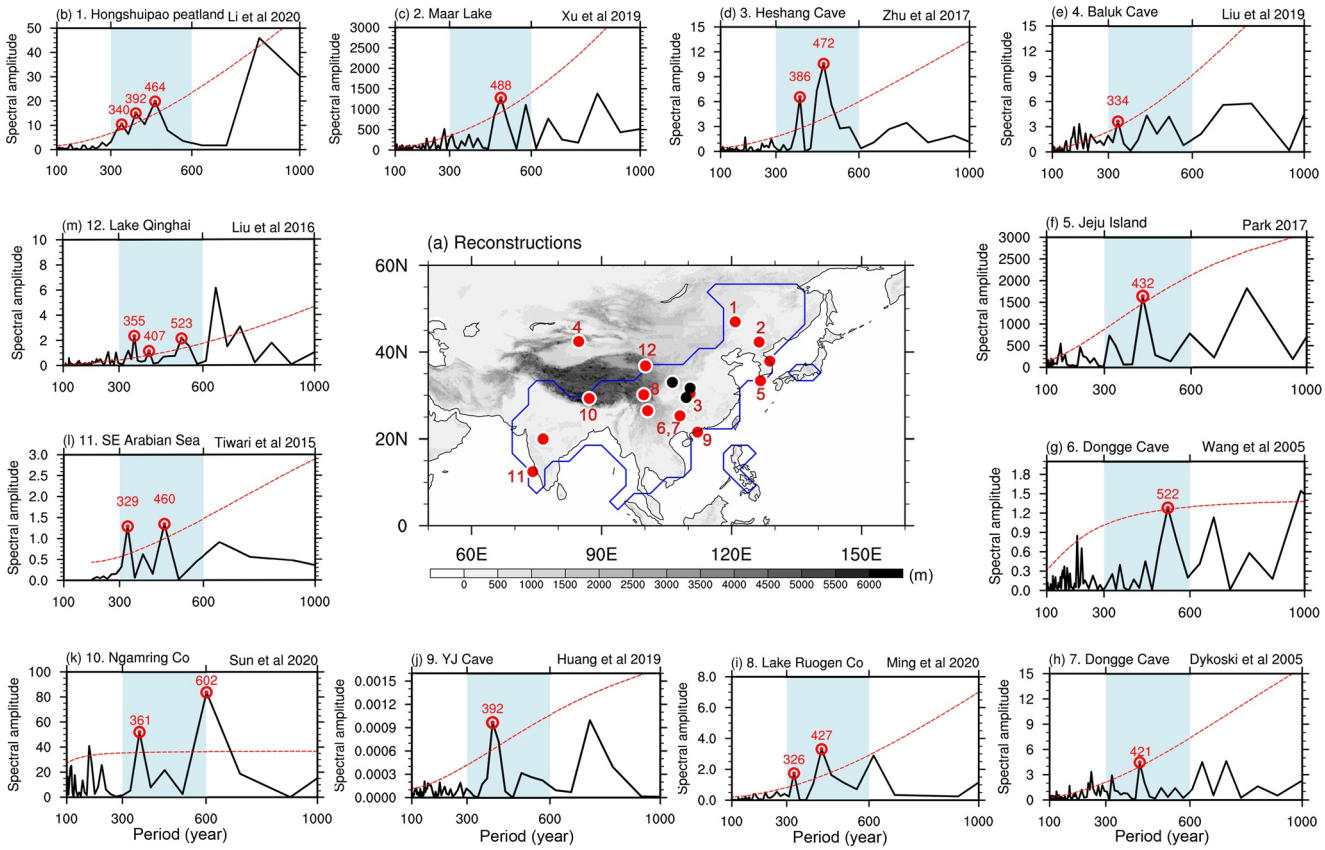

Figure 1. Periodicities of Asian dry/wet reconstructions during the Holocene. (a) Locations of reconstruction data used in this study (details shown in Table S1 in Supporting Information S1). Red dots denote that the reconstructions contain a 300–600-year cycle, otherwise they are marked as black. Blue lines outline the Asian summer monsoon (ASM) land region. (b–m) Power spectrum analysis of each reconstructed data set. The dashed red line in each panel represents the 90% confidence level. The blue shadings mark the 300–600-year cycle.

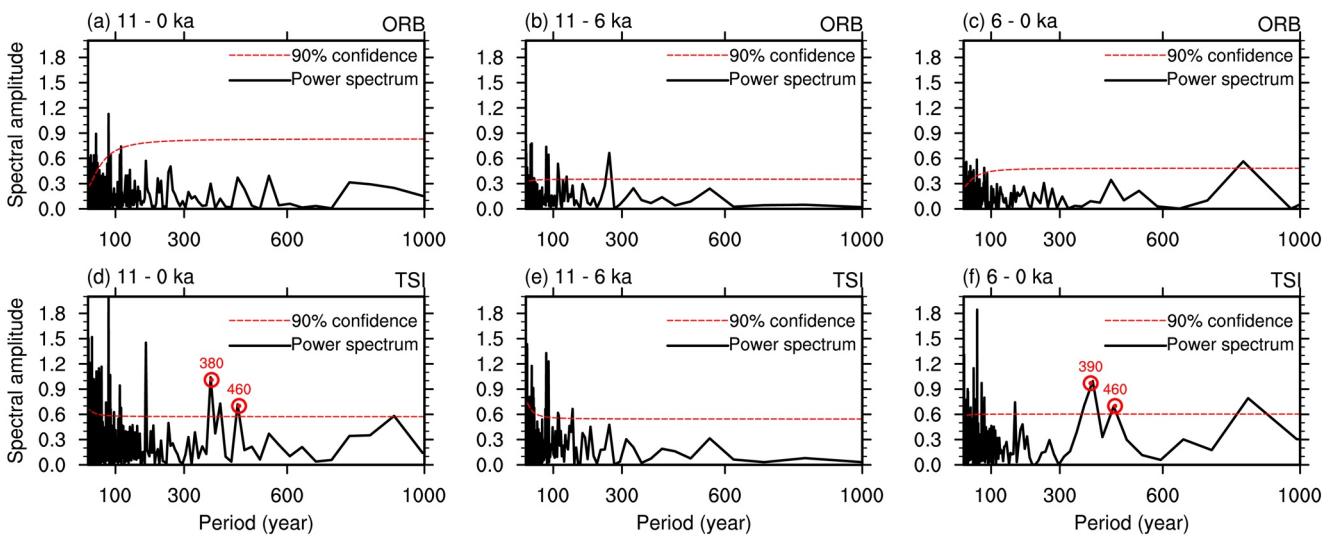

Figure 2. Simulated periodicities of Asian summer monsoon (ASM) land precipitation during the Holocene. Power spectrum analysis of June–July–August (JJA) ASM land precipitation during 11–0 ka (a), 11–6 ka (b), and 6–0 ka BP (c), respectively, under the impact of ORB. (d–f) are the same as (a–c), but under the impact of total solar irradiance (TSI). The analysis is performed on the unfiltered data. The dashed red line in each panel represents the 90% confidence level.

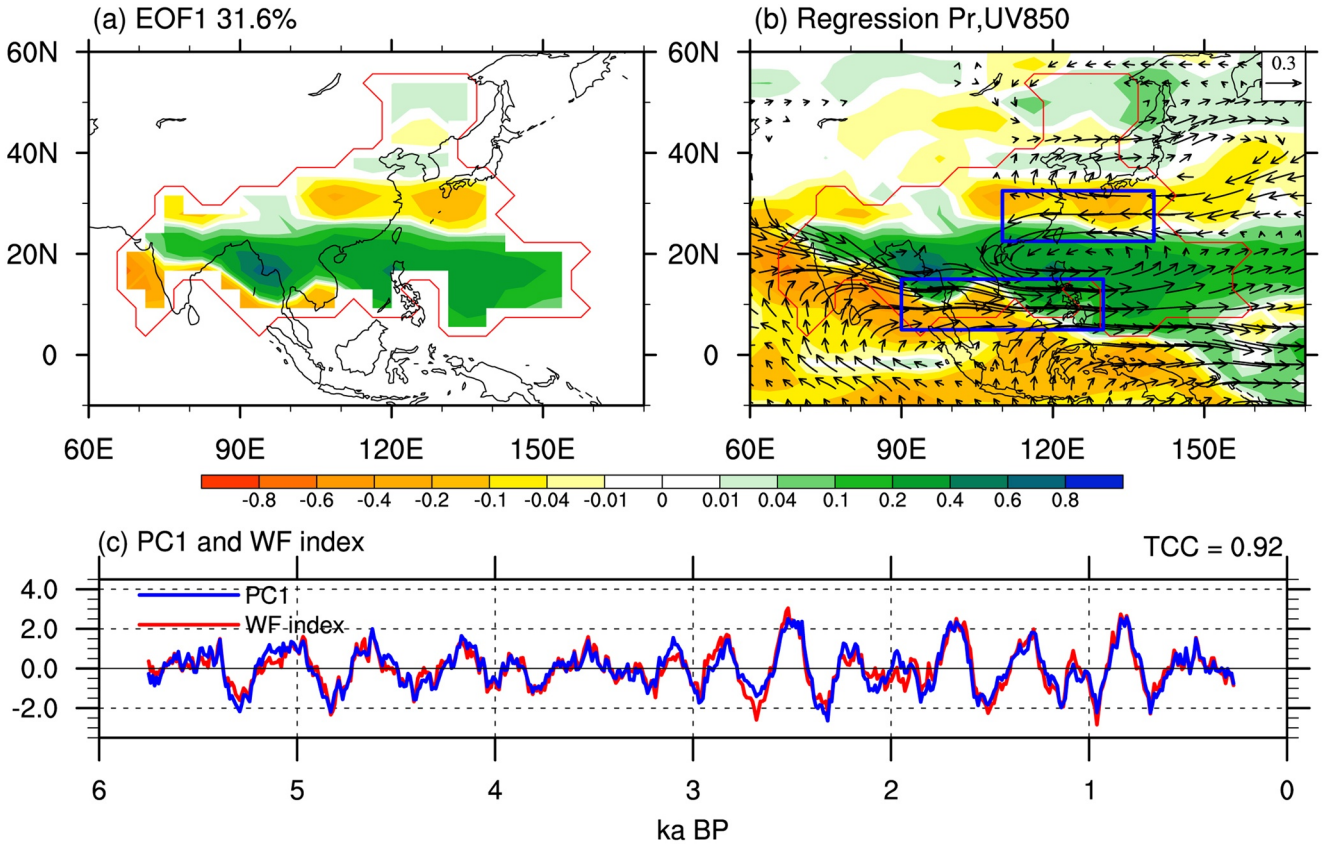

Figure 3. Spatial pattern of Asian summer monsoon (ASM) precipitation and circulation under the impact of total solar irradiance (TSI). (a) The EOF1 pattern of June–July–August (JJA) mean precipitation anomalies on a multi-centennial time scale during the period 6–0 ka BP. A method of subtracting the 400-year running mean from the 150-year running mean was applied before analysis. (b) Regressed JJA mean precipitation (mm day^{-1}, shading) and 850 hPa winds (m s^{-1}, vectors) on the normalized PC1. Only the significant results with confidence levels exceeding 90% (two-tailed Student's *t*-test) are displayed. Blue boxes represent the region of the Wang and Fan[36] index, which is defined by U850 in (5°–15°N, 90°–130°E) minus U850 in (22.5°–32.5°N, 110°–140°E). (c) Time series of PC1 (blue line) and WF index (red line). The correlation coefficient between the PC1 and WF index is 0.92.

380-year and 460-year cycles during the Holocene (Figure 2d), especially during the mid-late Holocene (Figure 2f), which is consistent with the proxy reconstructions. This result is similar to that in the TSI + ORB experiment (Figure not shown). We also examined the influence of other external forcings on multi-centennial ASM variability in the TraCE-21ka, where there was no solar activity change in the all-forcing or single-forcing experiments. No significant centennial to multi-centennial peaks in the ASM precipitation during the Holocene were found under the individual orbital, greenhouse gases, ice sheet, and melting water forcings, as well as in the all-forcing experiments (Figure S3 in Supporting Information S1). This implies that multi-centennial ASM variability is primarily affected by solar activity.

The spatial pattern of ASM variation on a multi-centennial time scale was investigated by utilizing the empirical orthogonal function (EOF) of ASM precipitation (Figure 3a). Under the influence of TSI, the EOF1 showed an overall zonally elongated "wet tropics–dry subtropics" pattern, with wet conditions over India and Southeast Asia while dry anomalies in central China, which is a characteristic feature of ASM across time scales (e.g., Wang et al., 2008). There was a more in-phase relationship between the Indian summer monsoon (ISM) and the Southeast Asian monsoon.

Further analysis of regressed precipitation and atmospheric circulation on the normalized PC1 suggested that the precipitation anomaly pattern was associated with the development of a zonally elongated cyclonic anomaly over the western North Pacific (WNP), along 20°N (Figure 3b). A pressure trough extends from the tropical WNP to northern India, enhancing the precipitation over the tropical Asia and WNP. The spatial patterns can be similar using a method of 300–600-year Lanczos bandpass filtering (Figure S4 in Supporting Information S1). We argue

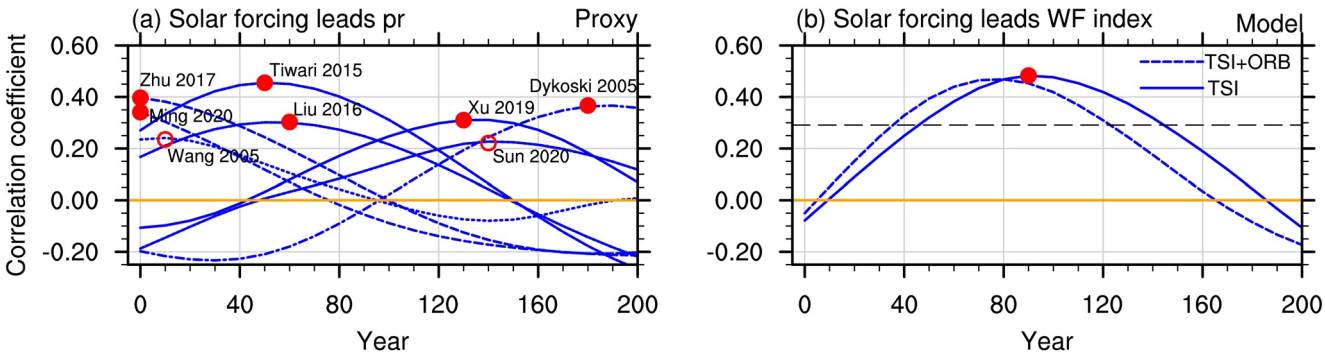

Figure 4. Impact of solar forcing on the temporal variation of Asian summer monsoon (ASM) during 6–0 ka BP. (a) Lead correlation coefficient between solar forcing and precipitation inferred by proxy data. Proxy data were linearly interpolated to 10-year resolution, and a method of subtracting the 400-year running mean from the 150-year running mean was applied before analysis. Proxy data of Dykoski et al. (2005), Tiwari et al. (2015), Wang et al. (2005), and Zhu et al. (2017) were multiplied by negative 1 to represent wet condition. Red filled circles mark the peak values of correlation coefficients, which are significant at the 90% confidence level (*r* test). (b) Lead correlation coefficient between solar forcing and WF index in the model simulation. The blue dashed line represents the result under TSI + ORB, while the blue solid line represent the result under total solar irradiance (TSI). The black dashed lines denote significance at the 90% confidence level (*r* test).

that this WNP cyclonic anomaly could be the key circulation system responsible for the centennial variation in ASM precipitation.

To measure the strength of the WNP cyclonic anomaly, we used the meridional shear vorticity index proposed by Wang & Fan (1999) (WF index hereafter), which is defined by U850 in (5°–15°N, 90°–130°E) minus U850 in (22.5°–32.5°N, 110°–140°E) (Figure 3b). This index depicts variations in the coupled EA monsoon system, comprising the WNP subtropical high, WNP monsoon trough, and the EA subtropical front (Wang et al., 2008). The WF index exhibited strong multi-centennial variations and the correlation coefficient between the PC1 of ASM precipitation and the WF index was 0.92 (Figure 3c). Both of the WF index and PC1 show the multi-centennial periodicities of 300–600 years during 6–0 ka BP (Figure not shown), which is similar to the solar forcing. Therefore, we use the WF index (the WNP cyclonic anomaly) as measures of ASM multi-centennial variation.

3.2. Solar Forcing Leads the ASM System

How are ASM precipitation and WNP circulation system related to the solar activity on the multi-centennial time scale? Figure 4 shows the lead-lag correlation coefficients between them. Precipitation inferred by different proxy data generally suggests a positive correlation with solar forcing on the multi-centennial time scale (Figure 4a). Specifically, proxy data show that solar forcing leads precipitation by about 50–60 years (Liu et al., 2016; Tiwari et al., 2015) or 130–180 years (Dykoski et al., 2005; Xu et al., 2019). However, some other proxy data show an apparent simultaneous correlation between the data of Zhu et al. (2017) and Ming et al. (2020) and solar activity.

In modeling results, a significant correlation appeared at year 50 and reached a peak at approximately year 90, implying that solar forcing leads the WF index by approximately 90 years. This result suggests that solar forcing may drive the multi-centennial WNP circulation and the associated ASM variation with a distinctive lead of 90 years (about one-quarter of the cycle). This simulated one-quarter-cycle delay between the ASM response and solar activity seems to resemble those between the multi-decadal and centennial variability and solar activity reflected in proxy data.

Similarly, on the multi-centennial time scale, previous modeling studies also found that ocean surface temperature lags the 90-year and 200-year solar forcing within 20 and 44 years, respectively, while a centennial delay occurs in the deep ocean (Seidenglanz et al., 2012). On the decadal time scale, some studies found an approximate quarter cycle delay in the climate system (e.g., NAO, European temperature, North Atlantic and tropical Pacific climate) under the 11-year solar cycle (Andrews et al., 2015; Shindell et al., 2020). Nevertheless, some high-resolution reconstructions have showed climatic lags of 10–30 years under the 200-year solar periodicity (Breitenmoser et al., 2012), which is less than a quarter cycle. Because a 10-year acceleration was used in our experiments, the phase lag can be exaggerated.

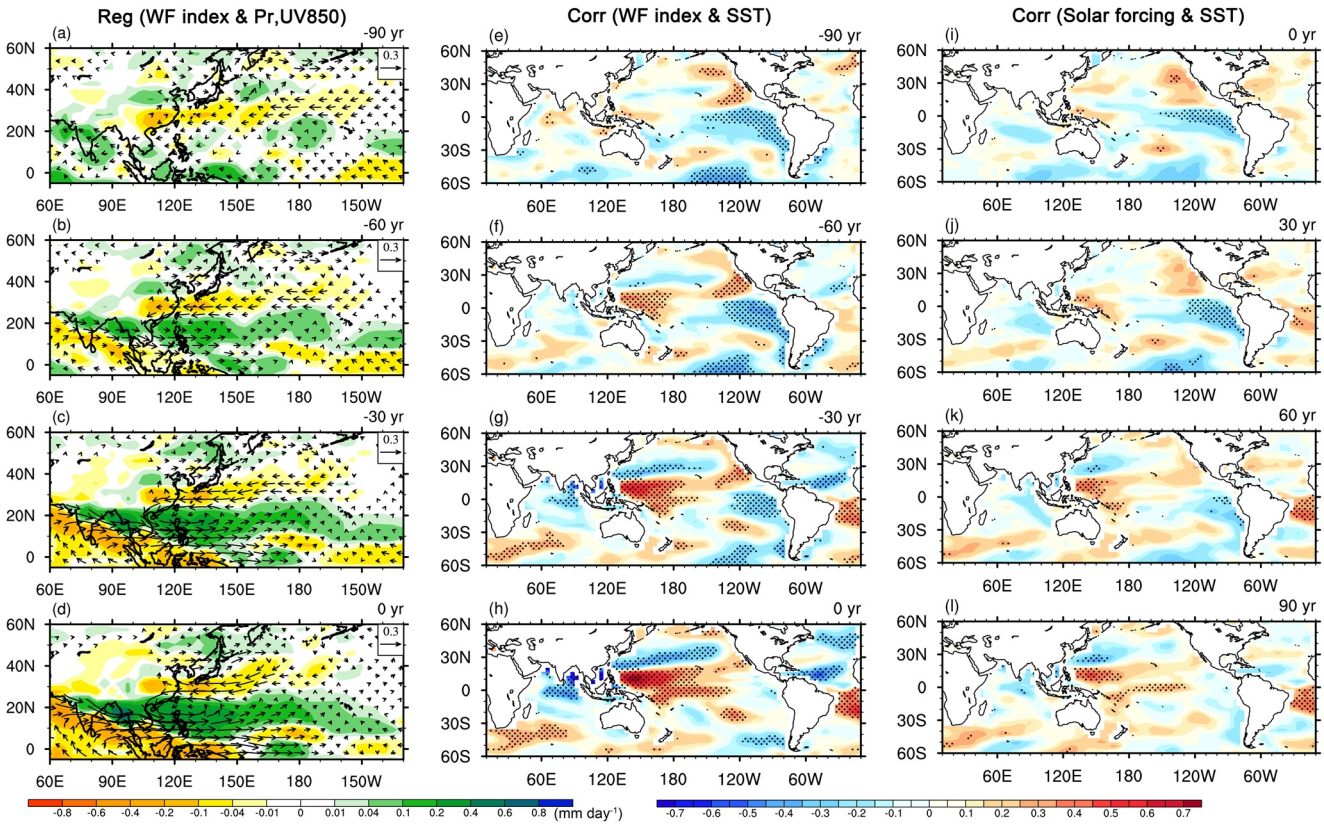

Figure 5. The spatial evolution of Asian summer monsoon (ASM) and the associated sea surface temperature (SST) pattern. (a–d) Regressed June–July–August (JJA) mean precipitation (mm day^{-1}, shading) and 850 hPa winds (m s^{-1}, vectors) on the normalized WF index. The labels "−30 years," "−60 years," and "−90 years" denote that the WF index lags precipitation and winds by 30, 60, and 90 years, respectively. Only the significant results with confidence levels exceeding 90% (two-tailed Student's *t*-test) are displayed. (e–h) Correlation maps of JJA mean SST (°C, shading) with the WF index. The dots denote results that are significant at the 90% confidence level (*r* test). (i–l) Correlation maps of JJA mean SST (°C, shading) with the solar forcing. The labels "30 years," "60 years," and "90 years" denote that the solar forcing leads SST by 30, 60, and 90 years, respectively.

To quantify the simulated monsoon response to solar irradiation change, we first checked the intensity of multi-centennial solar activity. During 6–0 ka BP, the intensity change of 300–600-year periodicity of solar activity was about 0.5 W m^{-2} (approximate 95% confidence intervals). Second, we used the 90-year-lag WF index, South Asian-western North Pacific (SA-WNP, 10°N–25°N, 75°E–160°E) precipitation, and central East Asian (EA) (25°N–35°N, 105°E–140°E) precipitation to represent the characteristics of the period with the strongest monsoon response to solar forcing (Figure S5 in Supporting Information S1). For an increase of 1 W m^{-2} total solar irradiance, the WF index and SA-WNP precipitation will increase about 1.91 m s^{-1} and 0.81 mm d^{-1}, respectively, while the central EA precipitation will decrease about −0.67 mm d^{-1}. This ASM response is larger than that under 11-year solar cycle in the solar-forcing runs in CESM-LME (Otto-Bliesner et al., 2016). It is also possible that the 10-year accelerated simulation might amplify this response.

3.3. Possible Mechanism of Multi-Centennial ASM Variation Under Solar Forcing

Next, we examined the multi-centennial spatial evolution of ASM precipitation and atmospheric circulation in the simulation. From year −90 to 0, the anomalous precipitation developed and wet conditions over a tropical rain belt extending from the Philippine Sea, via Southeast Asia, to northeastern India (Figures 5a–5d). There was a suppressed precipitation belt over subtropical EA, extending from the middle–lower reaches of the Yangtze River valley to southern Japan. This land part of the "wet tropics–dry subtropics" pattern closely resembled the EOF1 of the ASM precipitation (Figure 3a). Meanwhile, a deepened and northward shifted monsoon trough (convergence zone) caused enhanced moisture convergence and precipitation along 20°N from the WNP to northern India (Figures 5a–5d). Correspondingly, the subtropical high shifted northward and an anticyclonic anomaly

ridge was established along 35°N, extending from south of Japan westward to eastern China. This anomalous subtropical ridge suppresses EA subtropical frontal precipitation in the Yangtze River Valley and strengthens precipitation in northeast China. This coupled circulation pattern over the western Pacific–EA sector is also known as the Pacific–Japan pattern (Nitta, 1987). This meridional teleconnection pattern is accompanied by a local meridional circulation anomaly and a weakened upper-level subtropical westerly, which favors ascending motion over Northern China (Figure S6 in Supporting Information S1). The subtropical and extratropical precipitation anomalies arise from the meridional influence of tropical convective activities (Song et al., 2018; Wang et al., 2001). Thus, the delayed response of the prominent WNP anomalous cyclone can be responsible for the ASM precipitation on a multi-centennial time scale.

Because sea surface temperature (SST) could play an important role in modulating the WNP circulation systems, we analyzed the correlation map of global SST with the WF index (Figure 5e–5h). In general, the more significant correlation coefficient occurs in the tropical Pacific region from year −90 to 0. In year −90, cooling (negative correlation) occurs over the equatorial eastern Pacific, suggesting a La Niña-like Pacific SST pattern (Figure 5e). The anomalous 850 hPa winds are insignificant over the WNP region. From year −60 to 0, the SST warmed over the tropical western Pacific, increased precipitation and associated anomalous cyclone developed over the Philippine Sea (Figure 5f–5h). This WNP anomalous cyclone can be a Rossby wave response to the precipitation heating (Gill, 1980). This result indicates the important role of tropical western Pacific warming in developing the WNP cyclonic anomaly.

Then, the evolution of the "solar-related" SST anomalies was examined for comprehending this tropical SST response. We found the significant multi-centennial periodicities of the ENSO-like zonal SST gradient under the effect of TSI during the mid–late Holocene (Figure not shown), which is similar to the periodicities of solar forcing and simulated ASM variation. In the peaks of solar activity (year 0), significant cooling occurred over the equatorial eastern Pacific (Figure 5i), which was similar to the correlation map between SST and the WF index in year −90 (Figure 5e). For an increase of 1 W m^{-2} total solar irradiance, the Niño 3.4 index will decrease about 0.22°C, which can be similar to previous simulated result (e.g., Meehl & Arblaster, 2009; Meehl et al., 2009). We found that the strength of surface net downward heat flux can be negligible over the equatorial central-eastern Pacific, suggesting the role of ocean dynamics in causing the eastern Pacific SST cooling.

The "ocean thermostat" theory (Clement et al., 1996) might be responsible for the La Niña-like pattern at the solar peak. Solar forcing enhances the equatorial east–west SST gradient through enhancing the oceanic cold upwelling anomalies over the equatorial central eastern Pacific (Figure S7e in Supporting Information S1), which reduces the cold tongue SST. The enhanced zonal SST gradient induces anomalous equatorial easterlies and warms the western Pacific by thermocline adjustment, which in turn increases the SST gradient and activates the Bjerknes feedback (Figures S7a and S7b in Supporting Information S1). Meehl et al. (2003) found a solar-enhanced subtropical evaporation could intensify the Walker circulation, which may also enhance the La Niña-like pattern. Then, from year −60 to 0, warming over the western Pacific develops and induces the anomalous WNP cyclone (Figures S7b–S7d in Supporting Information S1). This mechanism was also found to be active during the Medieval Climate Anomaly (MCA) and the Little Ice Age (LIA) under solar-volcanic forcings (Liu et al., 2013; Mann et al., 2009).

Therefore, the solar-induced tropical SST and wind patterns (Figure 5i–5l and S7 in Supporting Information S1) are consistent with that during the development stage of ASM (Figure 5a–5h), confirming that solar activity modulates the tropical Pacific SST, developing an anomalous WNP cyclone, which causes a delayed ASM precipitation change.

4. Conclusion and Discussion

This work has investigated the impact of solar activity on ASM multi-centennial variation during the Holocene, based on orbital parameter and solar activity forcing experiments, multi-proxy records, and TraCE-21ka simulations. The transient simulation shows a clear 300–600-year cycle of ASM precipitation during the mid–late Holocene under the influence of TSI. This finding is supported by multiple high-resolution reconstructions. On the multi-centennial time scale, the leading mode of ASM variation shows a "wet tropics–dry subtropics" pattern, which lags solar activity by 90 years. The centennial variability of WNP cyclone is the critical circulation system responsible for the centennial ASM variability. The WNP anomalous cyclone, with a trough extending to

central India, enhances south Asia–WNP precipitation. It also results in the northward shift of the climatological subtropical high, weakening the upper-level subtropical westerly. It decreases precipitation over central China and increases precipitation over northeast China. The development of warm western tropical Pacific SST pattern is the essential cause of the anomalous WNP cyclone, which is modulated by solar forcing. Thus, we suggest that on the multi-centennial time scale, solar activity first modulates the tropical Pacific SST, which further develops the anomalous WNP cyclone and causes a delayed ASM response.

On the multi-centennial time scale, the overall spatial pattern of ASM precipitation is dominated by the "wet tropics–dry subtropics" pattern in the TSI experiment (Figure 3). The simulated ASM pattern is similar to reconstructions over southern Asia, the southeast Qinghai–Tibet Plateau, and northeast Asia, most of which suggest a 300–600-year cycle and correlate well with solar activity (e.g., Dykoski et al., 2005; Liu et al., 2016; Tiwari et al., 2015; Xu et al., 2019). However, the number of high-resolution reconstruction data is limited, and there is still some uncertainty in their correlation with solar activity. Moreover, the resolutions of model and multi-model ensembles need to be further developed in the future, which would be conducive to a more detailed description of physical processes and a reduction in uncertainty on a centennial time scale.

About 300 years have passed since the last solar minimum (Maunder grand solar minima, ~1,650–1,715), and now we are in the maximum solar period (Matthes et al., 2017). The empirical forecast predicted a similar solar irradiation minimum at the end of the 21st century (Abreu et al., 2008; Matthes et al., 2017). It means that the multi-centennial solar cycle might significantly impact the future climate. Thus, it is urgent to understand the impact of this multi-centennial solar cycle on the ASM variability, which might have significance for the long-term projection of future changes in the Asian monsoon.

Data Availability Statement

The GPCP observations are archived at https://www.esrl.noaa.gov/psd/data/gridded. The TraCE-21ka simulations are archived at https://www.earthsystemgrid.org. Modeling data supporting our findings can be found at https://doi.org/10.5281/zenodo.5782792. The proxy data are all derived from the previous published work, which can be downloaded at https://www.ncei.noaa.gov/products/paleoclimatology/climate-reconstruction (with a name search).

Acknowledgments
The authors thank the GPCP and TraCE-21ka for providing the observation and modeling data, and thank the researchers who provided the proxies (listed in Table S1 in Supporting Information S1). The authors study was supported by the National Natural Science Foundation of China (Grant Nos. 42130604, 42105044, 41971108, 42111530182, and 91437218) and Swedish STINT (Grant No. CH2019-8377).

References

Abreu, J. A., Beer, J., Steinhilber, F., Tobias, S. M., & Weiss, N. O. (2008). For how long will the current grand maximum of solar activity persist? *Geophysical Research Letters*, *35*(20), L20109. https://doi.org/10.1029/2008GL035442

Adler, R. F., Huffman, G., Chang, A., Ferraro, R., Xie, P., Janowiak, J. E., et al. (2003). The version 2 Global Precipitation Climatology Project (GPCP) monthly precipitation analysis (1979–present). *Journal of Hydrometeorology*, *4*(6), 1147–1167. https://doi.org/10.1175/1525-7541(2003)004<1147:TVGPCP>2.0.CO;2

Andrews, M. B., Knight, J. R., & Gray, L. J. (2015). A simulated lagged response of the North Atlantic Oscillation to the solar cycle over the period 1960–2009. *Environmental Research Letters*, *10*(5), 054022. https://doi.org/10.1088/1748-9326/10/5/054022

Bond, G., Kromer, B., Beer, J., Muscheler, R., Evans, M. N., Showers, W., et al. (2001). Persistent solar influence on North Atlantic climate during the Holocene. *Science*, *294*(5549), 2130–2136. https://doi.org/10.1126/science.1065680

Breitenmoser, P., Beer, J., Brönnimann, S., Frank, D., Steinhilber, F., & Wanner, H. (2012). Solar and volcanic fingerprints in tree-ring chronologies over the past 2000 years. *Palaeogeography, Palaeoclimatology, Palaeoecology*, *313–314*, 127–139. https://doi.org/10.1016/j.palaeo.2011.10.014

Bretherton, C. S., Widmann, M., Dymnikov, V. P., Wallace, J. M., & Bladé, I. (1999). The effective number of spatial degrees of freedom of a time-varying field. *Journal of Climate*, *12*(7), 1990–2009. https://doi.org/10.1175/1520-0442(1999)012<1990:TENOSD>2.0.CO;2

Cheng, J., Wu, H., Liu, Z., Gu, P., Wang, J., Zhao, C., et al. (2021). Vegetation feedback causes delayed ecosystem response to East Asian summer monsoon rainfall during the Holocene. *Nature Communications*, *12*(1), 1843. https://doi.org/10.1038/s41467-021-22087-2

Clement, A. C., Seager, R., Cane, M. A., & Zebiak, S. E. (1996). An ocean dynamical thermostat. *Journal of Climate*, *9*, 2190–2196. https://doi.org/10.1175/1520-0442(1996)009<2190:AODT>2.0.CO;2

Dong, S., & Ding, Y. (2016). Oceanic forcings of the interdecadal variability in east Asian summer rainfall. *Journal of Climate*, *29*(21), 763–764. https://doi.org/10.1175/JCLI-D-15-0792.1

Dykoski, C. A., Edwards, R. L., Cheng, H., Yuan, D., Cai, Y., Zhang, M., et al. (2005). A high-resolution, absolute-dated Holocene and deglacial Asian monsoon record from Dongge Cave, China. *Earth and Planetary Science Letters*, *233*(1–2), 71–86. https://doi.org/10.1016/j.epsl.2005.01.036

Gill, A. E. (1980). Some simple solutions for heat-induced tropical circulation. *Quarterly Journal of the Royal Meteorological Society*, *106*(449), 447–462. https://doi.org/10.1002/qj.49710644905

Goswami, B. N., Madhusoodanan, M. S., Neema, C. P., & Sengupta, D. A. (2006). Physical mechanism for North Atlantic SST influence on the Indian summer monsoon. *Geophysical Research Letters*, *33*(2), L02706. https://doi.org/10.1029/2005GL024803

He, C., Liu, Z., Otto-Bliesner, B. L., Brady, E. C., Zhu, C., Tomas, R., et al. (2021). Hydroclimate footprint of pan-Asian monsoon water isotope during the last deglaciation. *Science Advances*, *7*(4), eabe2611. https://doi.org/10.1126/sciadv.abe2611

Huang, C., Zeng, T., Ye, F., & Wei, G. (2019). Solar-forcing-induced spatial synchronisation of the East Asian summer monsoon on centennial timescales. *Palaeogeography, Palaeoclimatology, Palaeoecology*, *514*, 536–549. https://doi.org/10.1016/j.palaeo.2018.11.002

Li, N., Li, M., Sack, D., Kang, W., Song, L., Yang, Y., et al. (2020). Diatom evidence for mid-Holocene peatland water-table variations and their possible link to solar forcing. *Science of the Total Environment*, *725*, 138272. https://doi.org/10.1016/j.scitotenv.2020.138272

Liu, J., Wang, B., Cane, M. A., Yim, S., & Lee, J. (2013). Divergent global precipitation changes induced by natural versus anthropogenic forcing. *Nature*, *493*(7434), 656–659. https://doi.org/10.1038/nature11784

Liu, J., Wang, B., Ding, Q., Kuang, X., Soon, W., & Zorita, E. (2009). Centennial variations of the global monsoon precipitation in the last millennium: Results from ECHO-G model. *Journal of Climate*, *22*(9), 2356–2371. https://doi.org/10.1175/2008JCLI2353.1

Liu, X., Vandenberghe, J., An, Z., Li, Y., Jin, Z., Dong, J., & Sun, Y. (2016). Grain size of Lake Qinghai sediments: Implications for riverine input and Holocene monsoon variability. *Palaeogeography, Palaeoclimatology, Palaeoecology*, *449*, 41–51. https://doi.org/10.1016/j.palaeo.2016.02.005

Liu, Z., Otto-Bliesner, B. L., He, F., Brady, E. C., Tomas, R., Clark, P. U., et al. (2009). Transient simulation of last deglaciation with a new mechanism for Bølling-Allerød warming. *Science*, *325*(5938), 310–314. https://doi.org/10.1126/science.1171041

Liu, Z., Zhu, J., Rosenthal, Y., Zhang, X., Otto-Bliesner, B. L., Timmermann, A., et al. (2014). The Holocene temperature conundrum. *Proceedings of the National Academy of Sciences of the United States of America*, *111*(34), 3501–3505. https://doi.org/10.1073/pnas.1407229111

Lorenz, S. J., & Lohmann, G. (2004). Acceleration technique for Milankovitch type forcing in a coupled atmosphere-ocean circulation model: Method and application for the Holocene. *Climate Dynamics*, *23*(7–8), 727–743. https://doi.org/10.1007/s00382-004-0469-y

Lu, R., Dong, B., & Ding, H. (2006). Impact of the atlantic multidecadal oscillation on the Asian summer monsoon. *Geophysical Research Letters*, *33*(24), L24701. https://doi.org/10.1029/2006GL027655

Mann, M. E., Zhang, Z., Rutherford, S., Bradley, R. S., Hughes, M. K., Shindell, D., et al. (2009). Global signatures and dynamical origins of the little ice age and medieval climate anomaly. *Science*, *326*(5957), 1256–1260. https://doi.org/10.1126/science.1177303

Matthes, K., Funke, B., Szelag, M. E., Barnard, L., Beer, J., Charbonneau, P., et al. (2017). Solar forcing for CMIP6 (v3.2). *Geoscientific Model Development*, *10*(6), 2247–2302. https://doi.org/10.5194/gmd-10-2247-2017

Meehl, G. A., & Arblaster, J. M. (2009). A lagged warm event-like response to peaks in solar forcing in the Pacific region. *Journal of Climate*, *22*(13), 3647–3660. https://doi.org/10.1175/2009JCLI2619.1

Meehl, G. A., Arblaster, J. M., Matthes, K., Sassi, F., & Loon, H. (2009). Amplifying the Pacific climate system response to a small 11-year solar cycle forcing. *Science*, *325*(5944), 1114–1118. https://doi.org/10.1126/science.1172872

Meehl, G. A., Washington, W. M., Wigley, T. M. L., Arblaster, J. M., & Dai, A. (2003). Solar and greenhouse gas forcing and climate response in the 20th century. *Journal of Climate*, *16*(3), 426–444. https://doi.org/10.1175/1520-0442(2003)016<0426:SAGGFA>2.0.CO;2

Ming, G., Zhou, W., Cheng, P., Wang, H., Xian, F., Fu, Y., et al. (2020). Lacustrine record from the eastern Tibetan Plateau associated with Asian summer monsoon changes over the past ∼ 6 ka and its links with solar and ENSO activity. *Climate Dynamics*, *55*(5–6), 1075–1086. https://doi.org/10.1007/s00382-020-05312-4

Misios, S., Mitchell, D. M., Gray, L. J., Tourpali, K., Matthes, K., Hood, L., et al. (2016). Solar signals in CMIP-5 simulations: Effects of atmosphere-ocean coupling. *Quarterly Journal of the Royal Meteorological Society*, *142*(695), 928–941. https://doi.org/10.1002/qj.2695

Nitta, T. (1987). Convective activities in the tropical Western Pacific and their impact on the Northern Hemisphere summer circulation. *Journal of the Meteorological Society of Japan*, *65*(3), 373–390. https://doi.org/10.2151/jmsj1965.65.3_373

Novello, V., Vuille, M., Cruz, F. W., Strikis, N., Paula, M., Edwards, R. L., et al. (2016). Centennial-scale solar forcing of the South American Monsoon System recorded in stalagmites. *Scientific Reperts*, *6*(1), 24762. https://doi.org/10.1038/srep24762

Otto-Bliesner, B. L., Fasullo, J., Brady, E. C., Jahn, A., Landrum, L., Stevenson, S., et al. (2016). Climate variability and change since 850 CE: An ensemble approach with the community Earth system model. *Bulletin of the American Meteorological Society*, *97*(5), 735–754. https://doi.org/10.1175/bams-d-14-00233.1

Park, J. (2017). Solar and tropical ocean forcing of late-Holocene climate change in coastal East Asia. *Palaeogeography, Palaeoclimatology, Palaeoecology*, *469*, 74–83. https://doi.org/10.1016/j.palaeo.2017.01.005

Seidenglanz, A., Prange, M., Varma, V., & Schulzet, M. (2012). Ocean temperature response to idealized Gleissberg and de Vries solar cycles in a comprehensive climate model. *Geophysical Research Letters*, *39*(22), L22602. https://doi.org/10.1029/2012GL053624

Shi, H., Wang, B., Liu, J., & Liu, F. (2019). Decadal–multidecadal variations of Asian summer rainfall from the little ice age to the present. *Journal of Climate*, *32*(22), 7663–7674. https://doi.org/10.1016/10.1175/JCLI-D-18-0743.1

Shindell, D. T., Faluvegi, G., & Schmidt, G. A. (2020). Influences of solar forcing at ultraviolet and longer wavelengths on climate. *Journal of Geophysical Research: Atmospheres*, *125*(7), 031640. https://doi.org/10.1029/2019JD031640

Song, F., Leung, R., Lu, J., & Dong, L. (2018). Seasonally-dependent responses of subtropical highs and tropical rainfall to anthropogenic warming. *Nature Climate Change*, *8*(9), 787–792. https://doi.org/10.1038/s41558-018-0244-4

Steinhilber, F., Abreu, J., Beer, J., Brunner, I., Christl, M., Fischer, H., et al. (2012). 9, 400 years of cosmic radiation and solar activity from ice cores and tree rings. *Proceedings of the National Academy of Sciences of the United States of America*, *109*(16), 5967–5971. https://doi.org/10.1073/pnas.1118965109

Sun, W., Liu, J., Wang, B., Chen, D., Liu, F., Wang, Z., et al. (2019). A "La Niña-like" state occurring in the second year after large tropical volcanic eruptions during the past 1500 years. *Climate Dynamics*, *52*(12), 7495–7509. https://doi.org/10.1007/s00382-018-4163-x

Sun, W., Liu, J., & Wang, Z. Y. (2017). Simulation of centennial-scale drought events over eastern China during the past 1500 years. *Journal of Meteorological Research*, *31*(1), 17–27. https://doi.org/10.1007/s13351-017-6090-x

Sun, W., Wang, B., Zhang, Q., Pausata, F. S. R., Chen, D., Lu, G., et al. (2019). Northern Hemisphere land monsoon precipitation increased by the Green Sahara during middle Holocene. *Geophysical Research Letters*, *46*(16), 9870–9879. https://doi.org/10.1029/2019GL082116

Sun, Z., Yuan, K., Hou, X., Ji, K., Li, C., Wang, M., & Hou, J. (2020). Centennial-scale interplay between the Indian summer monsoon and the westerlies revealed from ngamring Co, southern Tibetan plateau. *The Holocene*, *30*(8), 1163–1173. https://doi.org/10.1177/0959683620913930

Tan, L., Cai, Y., Cheng, H., Edwards, R. L., Gao, Y., Xu, H., et al. (2018). Centennial-to decadal-scale monsoon precipitation variations in the upper Hanjiang River region, China over the past 6650 years. *Earth and Planetary Science Letters*, *482*, 580–590. https://doi.org/10.1016/j.epsl.2017.11.044

Tiwari, M., Nagoji, S. S., & Ganeshram, R. S. (2015). Multi-centennial scale SST and Indian summer monsoon precipitation variability since the mid-Holocene and its nonlinear response to solar activity. *The Holocene*, *25*(9), 1415–1424. https://doi.org/10.1177/0959683615585840

Vieira, L. E. A., Solanki, S. K., Krivova, N., & Usoskin, I. (2011). Evolution of the solar irradiance during the Holocene. *Astronomy and Astrophysics*, *531*, A6. https://doi.org/10.1051/0004-6361/201015843

Wagner, G., Beer, J., Masarik, J., Muscheler, R., Kubik, P. W., Mende, W., et al. (2001). Presence of the solar de vries cycle (∼205 years) during the last ice age. *Geophysical Research Letters*, *28*(2), 303–306. https://doi.org/10.1029/2000GL006116

Wang, B., Biasutti, M., Byrne, M. P., Castro, C., Chang, C.-P., Cook, K., et al. (2021). Monsoons climate change assessment. *Bulletin of the American Meteorological Society*, *102*(1), E1–E19. https://doi.org/10.1175/BAMS-D-19-0335.2

Wang, B., & Ding, Q. (2008). Global monsoon: Dominant mode of annual variation in the tropics. *Dynamics of Atmospheres and Oceans*, *44*(3–4), 165–183. https://doi.org/10.1016/j.dynatmoce.2007.05.002

Wang, B., & Fan, Z. (1999). Choice of South Asian summer monsoon indices. *Bulletin of the American Meteorological Society*, *80*(4), 629–638. https://doi.org/10.1175/1520-0477(1999)080<0629:COSASM>2.0.CO;2

Wang, B., Wu, R., & Fu, X. (2000). Pacific–East Asian teleconnection: How does ENSO affect east Asian climate? *Journal of Climate*, *13*(9), 1517–1536. https://doi.org/10.1175/1520-0442(2000)013<1517:PEATHD>2.0.CO;2

Wang, B., Wu, R., & Lau, K. M. (2001). Interannual variability of the Asian summer monsoon: Contrasts between the Indian and the Western North Pacific-East Asian monsoons. *Journal of Climate*, *14*(20), 4073–4090. https://doi.org/10.1175/1520-0442(2001)014<4073:IVOTAS>2.0.CO;2

Wang, B., Wu, Z., Li, J., Liu, J., Chang, C., Ding, Y., & Wu, G. (2008). How to measure the strength of the East Asian summer monsoon? *Journal of Climate*, *21*(17), 4449–4463. https://doi.org/10.1175/2008JCLI2183.1

Wang, Y., Cheng, H., Edwards, R. L., He, Y., Kong, X., An, Z., et al. (2005). The Holocene Asian monsoon: Links to solar changes and north atlantic climate. *Science*, *308*(5723), 854–857. https://doi.org/10.1126/science.1106296

Xu, D., Lu, H., Chu, G., Liu, L., Shen, C., Li, F., et al. (2019). Synchronous 500-year oscillations of monsoon climate and human activity in Northeast Asia. *Nature Communications*, *10*, 1–10. https://doi.org/10.1038/s41467-019-12138-0

Zhang, H., Yu, K., Zhao, J., Feng, Y., Lin, Y., Zhou, W., & Liu, G. H. (2013). East Asian summer monsoon variations in the past 12.5 ka: High-resolution δ18O record from a precisely dated aragonite stalagmite in central China. *Journal of Asian Earth Sciences*, *73*, 162–175. https://doi.org/10.1016/j.jseaes.2013.04.015

Zhang, J., Kong, X., Zhao, K., Wang, Y., Liu, S., Wang, Z., et al. (2020). Centennial-scale climatic changes in Central China during the Holocene climatic optimum. *Palaeogeography, Palaeoclimatology, Palaeoecology*, *558*, 109950. https://doi.org/10.1016/j.palaeo.2020.109950

Zhu, Z., Feinberg, J., Xie, S., Bourne-Worster, M. D., Huang, C., Hu, C., & Cheng, H. (2017). Holocene ENSO-related cyclic storms recorded by magnetic minerals in speleothems of central China. *Proceedings of the National Academy of Sciences of the United States of America*, *114*(5), 852–857. https://doi.org/10.1073/pnas.1610930114

References From the Supporting Information

Katsuki, K., Yang, D., Lim, J., Lee, J., Asahi, H., & Han, M. (2017). Multi-centennial-scale changes in East Asian typhoon frequency during the mid-Holocene. *Palaeogeography, Palaeoclimatology, Palaeoecology*, *476*, 140–146. https://doi.org/10.1016/j.palaeo.2017.04.004

Liu, X., Rao, Z., Shen, C., Liu, J., Chen, J., Chen, S., et al. (2019). Holocene solar activity imprint on centennial- to multidecadal-scale hydroclimatic oscillations in arid central Asia. *Journal of Geophysical Research: Atmospheres*, *124*(5), 2562–2573. https://doi.org/10.1029/2018JD029699

Menzel, P., Gaye, B., Mishra, P. K., Anoop, A., Basavaiah, N., Marwan, N., et al. (2014). Linking Holocene drying trends from Lonar Lake in monsoonal central India to North Atlantic cooling events. *Palaeogeography, Palaeoclimatology, Palaeoecology*, *410*, 164–178. https://doi.org/10.1016/j.palaeo.2014.05.044